Clays and Clay Minerals, Vol. 45, No. 1, 1–7, 1997.

HYDROTHERMAL CRYSTALLIZATION OF AMMONIUM-SAPONITE AT 200 °C AND AUTOGENOUS WATER PRESSURE†

ROLAND J. M. J. VOGELS,[1] JOHAN BREUKELAAR,[2] J. THEO KLOPROGGE,[3]‡
J. BEN H. JANSEN[4] AND JOHN W. GEUS[1]

[1]Department of Inorganic Chemistry, University of Utrecht, P.O. Box 80.083, 3508 TB Utrecht, The Netherlands

[2]SRTCA (Shell Research B.V.), P.O. Box 38000, 1030 BN Amsterdam, The Netherlands

[3]TNO–Institute of Applied Physics–TU Delft, Department of Inorganic Materials Chemistry, P.O. Box 595, 5600 AN Eindhoven, The Netherlands

[4]Bowagemi, Prinses Beatrixlaan 20, 3972 AN Driebergen, The Netherlands

Abstract—The effects of reaction time (2 to 72 h) and NH_4^+/Al^{3+} molar ratio (1.6, 2.4 and 3.2) on the hydrothermal synthesis of ammonium-saponites are investigated. The gels are obtained by mixing powders, resulting in a stoichiometric composition, $Mg_3Si_{3.4}Al_{0.6}O_{10}(OH)_2$, with aqueous ammonium solutions, with and without F, to result in initial NH_4^+/Al^{3+} molar ratios of 1.6, 2.4 and 3.2. The solid bulk products are characterized by X-ray diffraction (XRD), X-ray fluorescence (XRF) and scanning electron microscopy (SEM) combined with energy-dispersive X-ray (EDX) analysis. The cation exchange capacity (CEC) is determined with an ammonia selective electrode and the pH of the water from the first washing is measured. Ammonium-saponite is formed rapidly within 16 h. A higher NH_4^+/Al^{3+} molar ratio and the presence of F facilitate the crystallization of saponite. Small metastable amounts of bayerite, $Al(OH)_3$, are present at low NH_4^+/Al^{3+} molar ratios; after short reaction times, they disappear. During the first 4 h, the pH decreases rapidly, then drops slowly to a constant level of approximately 4.6 after 60 h. With increasing reaction time, saponite crystallites grow in the *ab* directions of the individual sheets with almost no stacking to thicker flakes. The NH_4^+ CEC of the solid products increases strongly within the first 24 h. A maximum of 53.3 meq/100 g is observed. The saponite yield increases from approximately 25% after 2 h to almost 100% after 72 h.

Key Words—Cation Exchange Capacity, Saponite, Synthesis, X-ray Diffraction, X-ray Fluorescence.

INTRODUCTION

In recent years, interest has increased in the synthesis of smectites such as beidellite (Plee et al. 1987; Schutz et al. 1987; Kloprogge, van der Eerden et al. 1990; Kloprogge, Jansen and Geus 1990), (fluor) hectorite (Shabtai et al. 1984; Sterte and Shabtai 1987) and saponite (Suquet et al. 1977; Kloprogge 1992; Kloprogge, Breukelaar, Jansen and Geus 1993; Kloprogge, Breukelaar, Wilson et al. 1993). The smectites can be applied as catalysts and molecular sieves because of their high purity and adjustable composition.

At temperatures ranging from 125 to 280 °C, Kloprogge (1992); Kloprogge, Breukelaar, Jansen and Geus (1993); and Kloprogge, Breukelaar, Wilson et al. (1993) have synthesized ammonium-saponite within 72 h. They proposed a crystallization model, in which the crystallization starts with the growth of individual sheets. During the synthesis, individual sheets apparently stack to form thick flakes, while lateral growth continues more slowly.

A major problem with the synthesis is the incorporation of Al into the saponite structure. Theory predicts all Al^{3+} to be present at the tetrahedral sites, replacing Si^{4+}. Actually, however, Al^{3+} is additionally built in at octahedral sites, instead of Mg^{2+}, and even at interlayer sites, instead of NH_4^+. The resulting incorporation of excess Al drastically alters the physicochemical properties of the saponite, such as layer charge, swelling, cation exchange and acidity. Incorporation of Al^{3+} at other than the tetrahedral sites can be avoided by raising the ammonium concentration.

The aims of this study are: 1) to characterize the ammonium-saponite crystallites grown for increasing periods of time at constant temperature and pressure, in order to elucidate the conditions for Al incorporation in octahedral and interlayer sites; 2) to monitor the development of the size and stacking of the individual sheets as a function of synthesis time to corroborate the sheet stacking model of Kloprogge (1992) and Kloprogge, Breukelaar, Jansen and Geus (1993); and 3) to force Al^{3+} exclusively into the tetrahedral sites and ammonium into the interlayer sites by varying the NH_4^+/Al^{3+} molar ratio and the starting chemicals, and by addition of F.

EXPERIMENTAL METHODS

Saponite Synthesis

Gels were prepared from homogeneous mixtures of stoichiometric amounts of the powdered compounds

† This paper is a joint contribution from the Debye Institute, Utrecht, and Shell Research B.V., Amsterdam, The Netherlands.

‡ Current address: Hoevenbos 299, 2716 Zoetermeer, The Netherlands.

https://doi.org/10.1346/CCMN.1997.0450101 Published online by Cambridge University Press

Table 1. List of compounds (mol oxide) used in the starting gels.

Sample	Amorph SiO_2	Silica/alumina		Altriiso-propoxide	$Al(NO_3)_3$	Mg acetate	$Mg(NO_3)_2$	$Mg(OH)_2$	NH_4OH	NH_4F
		SiO_2	Al_2O_3							
LTSAP8A	0.283	—	—	0.050	—	0.250	—	—	0.080	—
LTSAP9A	0.283	—	—	0.050	—	0.250	—	—	0.160	—
LTSAP10A	0.283	—	—	0.050	—	0.250	—	—	0.080	0.040
LTSAP11A	—	0.283	0.025	—	—	0.250	—	—	0.080	0.040
LTSAP12A	—	0.283	0.025	—	—	—	—	0.250	0.080	0.040
LTSAP13A	0.283	—	—	—	0.050	0.250	—	—	0.080	—
LTSAP14A	0.283	—	—	—	0.050	0.250	—	—	0.160	—
LTSAP15A	0.283	—	—	—	0.050	0.250	—	—	0.080	0.040
LTSAP16A	0.283	—	—	0.050	—	0.125	0.125	—	0.080	—
LTSAP17A	0.283	—	—	0.050	—	0.125	0.125	—	0.160	—
LTSAP18A	0.283	—	—	0.050	—	0.125	0.125	—	0.080	0.040
LTSAP19A	0.283	—	—	0.050	—	0.250	—	—	0.120	—
LTSAP20A	0.283	—	—	0.050	—	0.250	—	—	0.080	0.080

listed in Table 1, subsequently mixed with the desired amounts of aqueous solutions of ammonium chloride or ammonium fluoride. The Al compound was dissolved into the ammonium solution before mixing with the powdered Si and Mg compounds. Due to the high pH level of the ammonium solution, all dissolved Al^{3+} was fourfold coordinated, which is required for incorporation at tetrahedral sites in saponites. The theoretical composition of the ammonium-saponite is $(NH_4)_{0.6}Mg_3(Si_{3.4}Al_{0.6})O_{10}(OH)_2$. Table 1 lists the variation in compounds used for the preparation of the gels.

Approximately 125 g of the gel were hydrothermally treated in 250-mL Teflon beakers in autoclaves at 200 °C and autogenous water pressure (approximately 10–15 bar). After cooling, the solids were washed twice with demineralized water, followed by centrifugation. The pH of the coexisting hydrothermal fluid could not be determined, since the solid product had completely absorbed the fluid. Kloprogge (1992) and Kloprogge, Breukelaar, Jansen and Geus (1993) have shown that the pH of the hydrothermal fluid is only slightly lower than that of the water obtained from the first washing procedure. Therefore, the pH of the water of the first washing procedure was determined. The washed solid was suspended into 1 *M* ammonium chloride to ensure that all exchangeable sites were occupied by ammonium. Finally, the bulk solids were washed twice with demineralized water to remove excess ammonium chloride, sedimented by centrifugation and dried overnight at 120 °C.

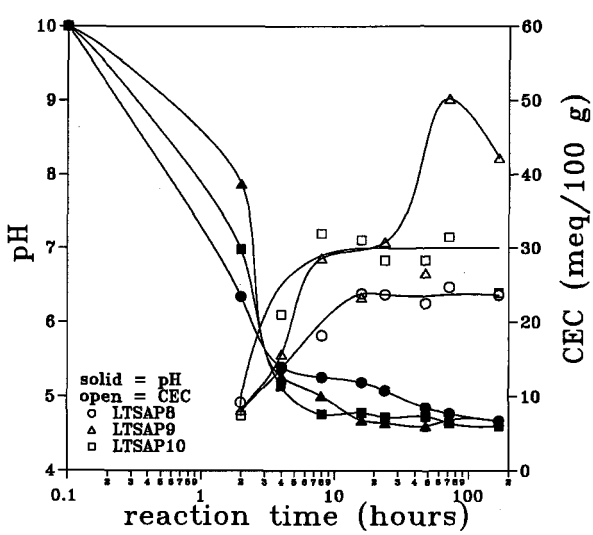

Figure 1. Decrease of pH (solid symbols) and development of the NH_4 CEC (open symbols) as function of synthesis time at 200 °C.

Analytical Techniques

X-ray powder diffraction patterns were recorded with a Philips diffractometer, equipped with PW 1700 hardware and APD 1700 software, using Cu*K*α radiation.

The CEC of the saponite was determined after exchange with 0.2 *M* NaCl by measuring the NH_4^+ content in the resulting solution with an ammonia-selective electrode. Saponites of LTSAP8A-7, LTSAP9A-7 and LTSAP10A-7 were exchanged with $Al(NO_3)_3$ instead of NaCl prior to XRF measurements.

Elemental analyses of Si, Al, Mg, N and F were performed on samples prepared according to the standard method used by the Koninklijke/Shell Laboratory Amsterdam (now called "SRTCA") by wavelength-dispersive XRF.

The morphology of the products obtained was investigated with a scanning electron microscope equipped with EDX analyzers.

RESULTS

Table 2 summarizes the pH of the fluid obtained from the first washing procedure, the cation (ammonium) CEC and the crystalline products. The pH decreases very rapidly during the first 16 h, followed by a slow decrease toward a constant value

https://doi.org/10.1346/CCMN.1997.0450101 Published online by Cambridge University Press

Table 2. Experimental runs at 200 °C and autogenous water pressure.

Run	Time h	NH_4/ Al	Fluor/ Al	pH†	CEC meq/ 100 g	Products‡
LTSAP8A-1	2	1.6		6.34	9.2	S BA
LTSAP8A-2	4	1.6		5.40	13.8	S BA
LTSAP8A-3	8	1.6		5.26	18.2	S
LTSAP8A-4	16	1.6		5.19	23.8	S
LTSAP8A-5	24	1.6		5.08	23.7	S
LTSAP8A-6	48	1.6		4.85	22.5	S
LTSAP8A-7	72	1.6		4.77	24.7	S
LTSAP8A-8	168	1.6		4.67	23.6	S
LTSAP9A-1	2	3.2		7.87	8.1	S
LTSAP9A-2	4	3.2		5.27	15.7	S
LTSAP9A-3	8	3.2		5.01	28.6	S
LTSAP9A-4	16	3.2		4.68	23.3	S
LTSAP9A-5	24	3.2		4.64	30.8	S
LTSAP9A-6	48	3.2		4.60	26.6	S
LTSAP9A-7	72	3.2		4.68	50.2	S
LTSAP9A-8	168	3.2		4.66	42.2	S
LTSAP10A-1	2	2.4	0.8	6.98	7.4	S F
LTSAP10A-2	4	2.4	0.8	5.14	21.0	S F
LTSAP10A-3	8	2.4	0.8	4.76	32.0	S
LTSAP10A-4	16	2.4	0.8	4.78	31.1	S F
LTSAP10A-5	24	2.4	0.8	4.72	28.3	S F
LTSAP10A-6	48	2.4	0.8	4.73	28.3	S F
LTSAP10A-7	72	2.4	0.8	4.64	31.5	S F
LTSAP10A-8	168	2.4	0.8	4.60	23.9	S F
LTSAP11A	72	2.4	0.8	4.86	53.3	S Q F
LTSAP12A	72	2.4	0.8	9.94	52.1	S Q F B
LTSAP13A	72	1.6		4.78	15.3	S L
LTSAP14A	72	3.2		4.65	18.8	S L
LTSAP15A	72	2.4	0.8	4.75	20.7	S L F
LTSAP16A	72	1.6		4.52	14.5	S L
LTSAP17A	72	3.2		4.53	18.6	S L
LTSAP18A	72	2.4	0.8	4.41	19.1	S L F
LTSAP19A	72	2.4		4.51	21.9	S L
LTSAP20A	72	1.6	1.6	4.62	32.4	S L F

† Measured after the first washing.
‡ S = saponite, F = sellaite, Q = quartz, L = lizardite, B = brucite, BA = bayerite and all experiments contain various amounts of amorphous material.

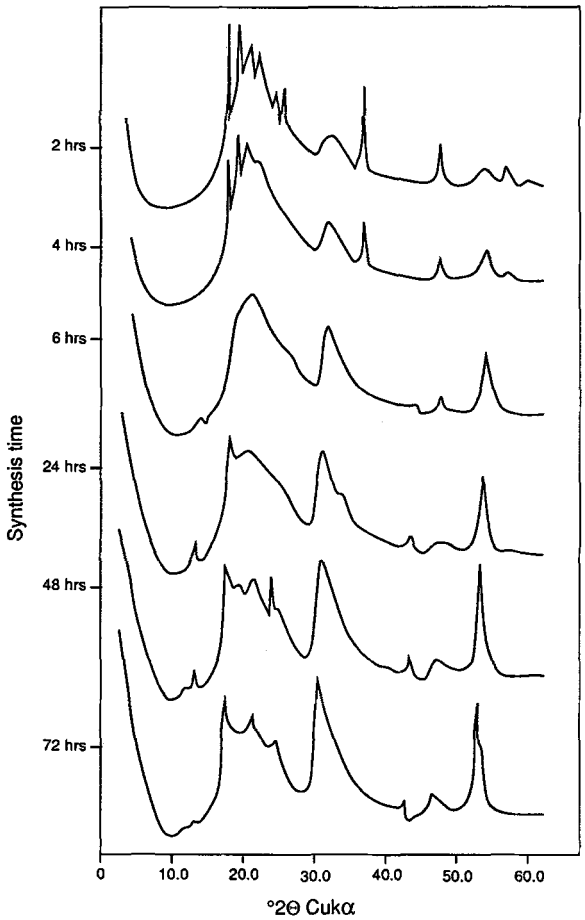

Figure 2. X-ray powder diffraction patterns with increasing synthesis time at 200 °C; LTSAP8A.

of approximately 4.6 upon prolonged synthesis time (Figure 1). The pH of LTSAP12A (Table 2), 9.94, is very high when compared to that of all other experiments. The pH values of the series LTSAP16A, LTSAP17A, LTSAP18A and LTSAP19A are slightly lower as compared to those measured with the other experiments.

The NH_4-CEC values are low, never representing more than 35% of the theoretical CEC of 155 meq/100 g for pure ammonium-saponite. The CEC increases strongly within the first 24 h, while longer synthesis times result in essentially constant CEC values (Figure 1). The very high (> 50 meq/100 g) CEC values for LTSAP9A-7, LTSAP11A and LTSAP12A are remarkable. Exchange of ammonium for aluminum instead of sodium results in an additional lowering of the NH_4-CEC to values of approximately 3.4 meq/100 g.

The XRD patterns display the development of the saponite structure with increasing synthesis time (Figure 2). LTSAP8A (Figure 2a) exhibits bayerite after 2 h, with poorly formed crystals of saponite. After 4 h, the amount of bayerite has decreased, and the bayerite diffraction maxima have completely disappeared after 8 h. The XRD patterns show that the (060) saponite reflection increases in relative intensity and sharpens during the first 48 h. With long periods of hydrothermal treatment, the (060) reflection remains constant, while the other (*hkl*) reflections sharpen. LTSAP9A shows a much faster development of saponite than LTSAP8A; XRD intensities of saponite in LTSAP9A-1 (2 h) can be compared with those of LTSAP8A-4 (16 h). LTSAP10A is intermediate in-between LTSAP8A and LTSAP9A.

Sellaite, MgF_2, is observed in all patterns independent of the synthesis time, due to the presence of F. In LTSAP10A, no bayerite is found. The XRD pattern of LTSAP12A also reveals quartz and brucite as secondary products together with very well-crystallized saponite (Figure 3a). LTSAP11A contains quartz as a sec-

https://doi.org/10.1346/CCMN.1997.0450101 Published online by Cambridge University Press

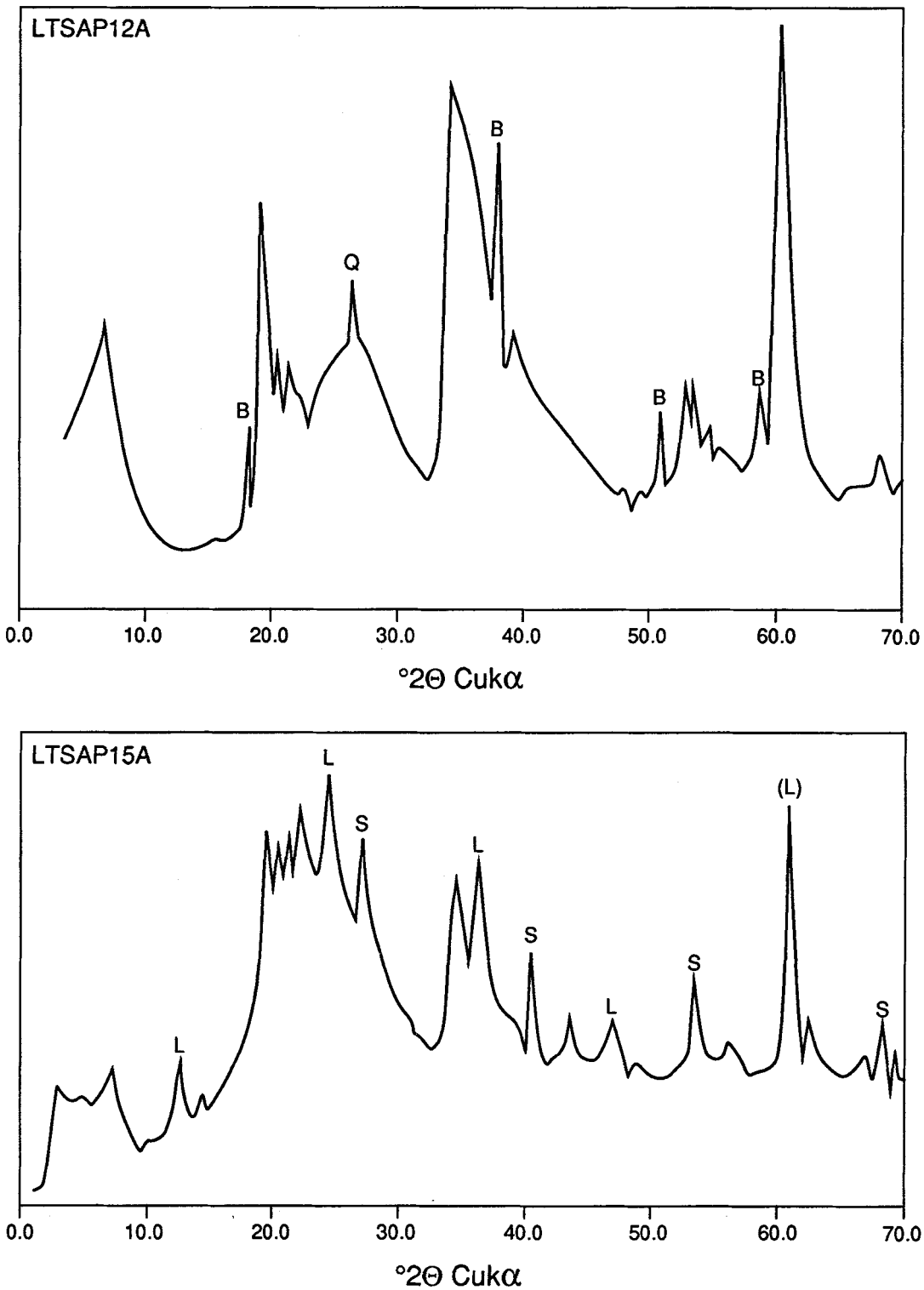

Figure 3. X-ray powder diffraction patterns of a) LTSAP12A and b) LTSAP15A. Q = quartz, B = brucite, S = sellaite, L = aluminum-lizardite.

https://doi.org/10.1346/CCMN.1997.0450101 Published online by Cambridge University Press

Table 3. XRF analyses of the run products.

Sample	MgO wt.%	Al_2O_3 wt.%	SiO_2 wt.%	N_{CEC} wt.%	N_{XRF} wt.%	F wt.%	Si/Al
LTSAP8A-1	6.05	10.20	67.71	0.13	0.17	na†	5.86
LTSAP8A-2	7.59	7.43	72.27	0.19	0.25	na	8.60
LTSAP8A-3	8.80	5.02	48.32	0.25	0.35	na	7.52
LTSAP8A-4	9.25	5.93	51.37	0.33	0.37	na	7.65
LTSAP8A-5	13.10	6.56	67.77	0.33	0.35	na	9.13
LTSAP8A-6	18.14	8.20	62.00	0.32	0.30	na	6.68
LTSAP8A-7	18.37	6.86	60.63	0.35	0.30	na	7.81
LTSAP8A-8	20.23	8.90	54.83	0.33	0.29	na	5.44
LTSAP9A-1	12.62	10.75	60.27	0.11	0.16	na	4.95
LTSAP9A-2	18.06	8.90	58.62	0.22	0.22	na	5.82
LTSAP9A-3	23.96	8.12	51.45	0.40	0.57	na	5.59
LTSAP9A-4	24.53	8.01	51.26	0.33	0.45	na	5.65
LTSAP9A-5	22.64	7.48	47.34	0.43	0.47	na	5.59
LTSAP9A-6	19.48	8.69	55.15	0.37	0.37	na	5.60
LTSAP9A-7	23.91	7.92	50.64	0.70	0.72	na	5.65
LTSAP9A-8	24.63	7.80	54.64	0.59	0.59	na	6.18
LTSAP10A-1	8.42	10.37	66.13	0.10	0.15	2.89	5.63
LTSAP10A-2	16.48	8.77	59.94	0.29	0.36	na	6.04
LTSAP10A-3	22.30	8.43	56.44	0.45	0.48	na	5.91
LTSAP10A-4	22.44	8.69	55.54	0.44	0.50	2.35	5.64
LTSAP10A-5	23.02	8.46	55.75	0.40	0.47	na	5.82
LTSAP10A-6	22.73	8.99	53.76	0.40	0.42	2.38	5.28
LTSAP10A-7	23.96	8.50	53.03	0.44	0.47	na	5.51
LTSAP10A-8	23.95	8.37	52.61	0.33	0.43	na	5.55
LTSAP11A	19.02	11.22	54.49	0.75	na	na	4.29
LTSAP12A	30.26	8.80	43.58	0.73	na	na	4.37
LTSAP13A	8.99	10.66	68.63	0.21	na	na	5.69
LTSAP14A	17.46	9.58	61.27	0.26	na	na	5.65
LTSAP15A	12.90	10.17	65.34	0.29	na	na	5.68
LTSAP16A	15.87	9.50	61.53	0.20	na	na	5.72
LTSAP17A	19.87	8.82	56.50	0.26	na	na	5.66
LTSAP18A	18.90	8.96	58.06	0.27	na	na	5.73
LTSAP8A-7E‡	18.13	8.56	61.14	0.13	na	na	6.31
LTSAP9A-7E‡	22.44	9.95	50.64	0.14	na	na	4.49
LTSAP10A-7E‡	22.36	9.48	51.79	0.13	na	na	4.82
Theory§	31.04	7.86	52.47	2.16			5.67

† na = not analyzed.
‡ Samples with the extension "E" represent analyses after exchange with aluminum nitrate.
§ Theoretical saponite composition $(NH_4)_{0.6}Mg_3Si_{3.4}Al_{0.6}O_{10}(OH)_2$, which was intended in the bulk chemistry of the gel.

ondary product. The saponites of LTSAP13A, LTSAP14A and LTSAP15A contain many defects or are very small crystallites. These series contain a second sheet silicate, aluminum-lizardite $(Mg,Al)_3(Si,Al)_2O_5(OH)_4$, whereas LTSAP15A also contains a relatively large amount of sellaite (Figure 3b). The XRD patterns of LTSAP16A, LTSAP17A and LTSAP18A are largely comparable with those of LTSAP13A, LTSAP14A and LTSAP15A.

The XRF analyses (Table 3) reveal a systematic change in bulk composition with synthesis time. During the first 8 h, SiO_2 and Al_2O_3 decrease, whereas MgO and N increase. Longer synthesis times have no influence on the composition within the series LTSAP9A and LTSAP10A. For LTSAP8A, SiO_2 and Al_2O_3 continue to drop and MgO and N to increase slowly with time. The increase of the N content of the solids runs more or less parallel with the rise in CEC, although the CEC is always lower than the analytically assessed N content. The XRF analyses after cation exchange of Al^{3+} for $[NH_4]^+$ display only a slight decrease of Mg.

SEM (Figure 4) illustrates 2 examples of the products formed after 72 h (LTSAP8A-7, LTSAP9A-7, LTSAP12A, LTSAP14A and LTSAP19A). All samples consist of large (up to 100 μm) amorphous particles overgrown with clusters of small flakes (diameter < 10 μm). Some smooth flakes have a diameter > 20 μm. The EDX analyses, although providing only relative amounts, reveal that the large amorphous particles contain only SiO_2, with some MgO on their surfaces. The large flakes consist of SiO_2, Al_2O_3 and MgO of a weight ratio of 3:0.5:1. The small flakes also contain SiO_2, Al_2O_3 and relatively more MgO as compared to the large flakes.

https://doi.org/10.1346/CCMN.1997.0450101 Published online by Cambridge University Press

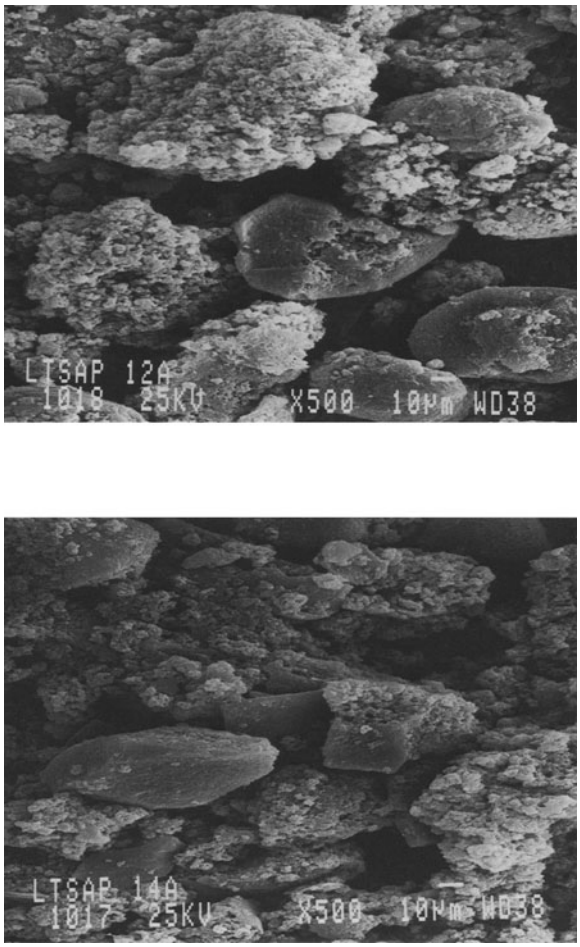

Figure 4. SEM photographs of LTSAP12A and LTSAP14A.

DISCUSSION

The synthesis of ammonium-saponite was successful in all experiments, although the amount formed and the sharpness of the XRD patterns depended strongly upon synthesis time, ammonium concentration and the constituents of the initial gels.

During the first 4 h of the hydrothermal treatment, the pH decreases sharply, due to the release of mainly acetate ions, while part of the Mg is incorporated into the crystallizing saponite. After 4 h, the pH has reached levels between 6.4 and 5.4, the exact range in which $Al(OH)_3$ has its minimum solubility (Hem and Roberson 1967). The drop in pH explains the formation of bayerite in LTSAP8A-1 and LTSAP8A-2. After 8 more h, the bayerite disappears as a separate phase. The bayerite may dissolve due to the removal of Al from the solution by incorporation of octahedral Al into the saponite structure. Alternatively, the small bayerite units may be incorporated as a kind of octahedral building unit. The second alternative is favored, because $Al(OH)_3$ has a very low solubility when the pH is between 6.4 and 5.4 (Hem and Roberson 1967). The incorporation of octahedral Al in the saponite structure, as established by Kloprogge (1992); Kloprogge, Breukelaar, Jansen and Geus (1993); and Kloprogge, Breukelaar, Wilson et al. (1993), is caused by the formation of bayerite during the first hours of the hydrothermal treatment. It has been suggested that the formation of bayerite is due to the fact that the Al of the isopropoxide remains sixfold coordinated during gelling. The series LTSAP8 shows that the incorporation is not prevented by dissolving the Al compound in basic ammonium solution, which forces the Al^{3+} into a tetrahedral coordination, before being mixed with the other compounds in the gel preparation method.

In the series LTSAP9A and LTSAP10A, no bayerite is observed. The very rapid crystallization of saponite and the resulting drop in pH to levels below 5.3 within the first 4 h may prevent the formation of bayerite or, alternatively, the initially formed bayerite has already disappeared after 2 h.

Based on the fact that magnesium nitrate and acetate are highly soluble within the observed pH range and assuming that almost all Mg apparent in the XRF bulk analyses has been incorporated into the octahedral sites of the saponite structure, one may calculate the saponite yield in the solid products (Table 4) with the data of Kloprogge, Breukelaar, Jansen and Geus (1993) for pure ammonium-saponite of identical compositions. After correction for adsorbed water, their pure ammonium-saponite contains 17.07 wt% Mg (31.04 wt% MgO). The trend of increasing percentages with increasing synthesis time runs parallel with the increase in CEC of the bulk product.

The use of $Mg(OH)_2$ in LTSAP12A resulted in the high pH levels observed. The high pH adversely affects the saponite crystallinity. The presence of brucite, which is due to the low solubility of magnesium hydroxide, explains the high Mg content observed with the XRF.

The decreasing differences in N contents, based on XRF and CEC determinations with increasing synthesis time, indicates that a part of the ammonium resides in nonexchangeable sites, or possibly amorphous material, which agrees with the data of Kloprogge (1992) and Kloprogge, Breukelaar, Jansen and Geus (1993).

The data of this study point to the following crystallization model. The saponite crystallization starts with the formation of separate sheets with hexametric rings containing Si and Al in distributions determined by the Loewenstein rule (Loewenstein 1954) together with bayerite. During the first period, the separate sheets grow mainly in the *ab* directions. Meanwhile, the bayerite sheets are incorporated as building units, instead of brucite sheets, into the saponite structure, resulting in a considerable amount of octahedral Al and the absence of Mg in the saponite structure. Later, stacking occurs as indicated by the increasing inten-

https://doi.org/10.1346/CCMN.1997.0450101 Published online by Cambridge University Press

Table 4. Ammonium-saponite content (in %) of the solid product determined from the Mg content and corresponding CEC values for the ammonium-saponite.

Sample	Sap %	NH_4-CEC meq/100 g
LTSAP8A-1	25.2	36.5
LTSAP8A-2	30.4	45.4
LTSAP8A-3	34.8	52.3
LTSAP8A-4	48.2	49.4
LTSAP8A-5	51.9	45.7
LTSAP8A-6	70.7	31.8
LTSAP8A-7	73.5	33.6
LTSAP8A-8	82.5	28.6
LTSAP9A-1	52.3	15.5
LTSAP9A-2	72.5	21.7
LTSAP9A-3	97.7	29.3
LTSAP9A-4	99.5	23.4
LTSAP9A-5	99.4	31.0
LTSAP9A-6	80.1	33.2
LTSAP9A-7	98.7	50.9
LTSAP9A-8	96.3	43.8
LTSAP10A-1	34.6	21.4
LTSAP10A-2	66.7	31.5
LTSAP10A-3	87.5	36.6
LTSAP10A-4	88.4	35.2
LTSAP10A-5	90.0	31.4
LTSAP10A-6	90.7	31.2
LTSAP10A-7	95.5	33.0
LTSAP10A-8	96.0	24.9

sities of the (*hkl*) reflections relative to (060). The low NH_4-CEC values indicate the presence of other interlayer cations, most probably Al. This is supported by the XRF analyses, which exhibit low MgO and high Al_2O_3 contents as compared to the theoretical values. The cation exchange experiments with aluminum nitrate result in nearly no exchange of Mg, demonstrating that practically no Mg was available as an interlayer cation. This model is largely in accordance with the model proposed by Kloprogge (1992); Kloprogge, Breukelaar, Jansen and Geus (1993); and Kloprogge, Breukelaar, Wilson et al. (1993), who established the exact Al distribution with ^{27}Al and ^{29}Si MAS-NMR.

CONCLUSIONS

1) The crystallinity of synthetic ammonium-saponite depends strongly on synthesis time, ammonium concentration and initial constituents of the gel.
2) During the synthesis, the pH decreases strongly due to the formation of acetic acid, which results in the formation of bayerite.
3) The use of magnesium hydroxide leads to an almost constantly high pH level, which leads to the presence of brucite in the solid products due to its low solubility.
4) A crystallization model is proposed in which: 1) separate sheets with hexametric rings containing Si and Al are formed, followed by lateral growth; 2) incorporation of bayerite as an octahedral building unit proceeds; 3) separate sheets are subsequently stacked; and 4) remaining Al from the solution is incorporated as interlayer cations together with a small amount of ammonium.

ACKNOWLEDGMENTS

The authors wish to thank A. de Winter for his help and advice in the laboratory.

REFERENCES

Hem JD, Roberson CE. 1967. Form and stability of aluminum hydroxide complexes in dilute solutions. USGS Water-Supply Paper 1827-A. Washington: US GPO. p 1–55.

Kloprogge JT. 1992. Pillared clays: Preparation and characterization of clay minerals and aluminum-based pillaring agents. Geologica Ultraiectina 91 [Ph.D. thesis] Utrecht, The Netherlands: Univ of Utrecht. 349 p.

Kloprogge JT, Breukelaar J, Jansen JBH, Geus JW. 1993. Development of ammonium-saponites from gels with variable ammonium concentration and water content at low temperatures. Clays Clay Miner 41:103–110.

Kloprogge JT, Breukelaar J, Wilson AE, Geus JW, Jansen JBH. 1993. Solid-state nuclear magnetic resonance spectroscopy on synthetic ammonium/aluminum saponites. Clays Clay Miner 42:416–420.

Kloprogge JT, van der Eerden AMJ, Jansen JBH, Geus JW. 1990. Hydrothermal synthesis of Na-beidellite. Geol Mijnbouw 69:351–357.

Kloprogge JT, Jansen JBH, Geus JW. 1990. Characterization of synthetic Na-beidellite. Clays Clay Miner 38:409–414.

Loewenstein W. 1954. The distribution of aluminum in the tetrahedra of silicates and aluminates. Am Mineral 39:92–96.

Plee D, Gatineau L, Fripiat JJ. 1987. Pillaring processes of smectites with and without tetrahedral substitution. Clays Clay Miner 35:81–88.

Schutz A, Stone WEE, Poncelet G, Fripiat JJ. 1987. Preparation and characterization of bidimensional zeolitic structures obtained from synthetic beidellite and hydroxy-aluminum solutions. Clays Clay Miner 35:251–261.

Shabtai J, Rosell M, Tokarz M. 1984. Cross-linked smectites: III. Synthesis and properties of hydroxy-aluminum hectorites and fluorhectorites. Clays Clay Miner 32:99–107.

Sterte J, Shabtai J. 1987. Cross-linked smectites: V. Synthesis and properties of hydroxy-silicoaluminum montmorillonites and fluorhectorites. Clays Clay Miner 35:429–439.

Suquet H, Iiyama JT, Kodama H, Pézerat H. 1977. Synthesis and swelling properties of saponites with increasing layer charge. Clays Clay Miner 25:231–242.

(Received 7 January 1993; accepted 24 August 1994; Ms. 2312)